

# Correlation of capacitance and actuation in ionomeric polymer transducers

B. J. AKLE\*, D. J. LEO

*Center for Intelligent Material Systems and Structures, Mechanical Engineering Department, Virginia Tech, Blacksburg, VA 24061-0261, USA*

M. A. HICKNER, J. E. MCGRATH

*Materials Research Institute, Chemistry Department, Virginia Tech, Blacksburg, VA 24061, USA*

Ionomeric polymer transducers are electromechanical actuators fabricated from ion-exchange membranes that have been surface plated with conductive metal. In this paper we discuss a series of experiments that characterize the electromechanical actuation response of three families of ionomers: Nafion (a product of DuPont), BPSH (sulfonated poly(arylene ether sulfone)) and PATS (poly(arylene thioether sulfone)). The first polymer is commercially-available while the second and third polymers are synthesized by the direct polymerization of sulfonated monomers in our lab. The mechanical properties and actuation response of Nafion-117, BPSH, and PATS of varying ionic content are studied in the Lithium cation form. The strain response of the materials varies from 50  $\mu\text{strain/V}$  to 750  $\mu\text{strain/V}$  at 1Hz. A linear correlation was found between the strain response and the capacitance of the material. This correlation was independent of the polymer composition and the plating parameters. All of the ionomers analyzed in this work exhibited a strain-to-charge response between 9  $\frac{\mu\text{strain}}{\frac{\text{C}}{\text{m}^2}}$  and 15  $\frac{\mu\text{strain}}{\frac{\text{C}}{\text{m}^2}}$ . Due to the fact that the low-frequency capacitance of an ionomer is strongly related to charge accumulation at the blocking electrodes, this correlation suggests a strong relationship between surface charge accumulation and mechanical deformation in ionomeric actuators.

© 2005 Springer Science + Business Media, Inc.

## 1. Introduction

Ionomeric polymer transducers consist of an ion-exchange membrane plated with conductive metal layers on the outer surfaces. Such materials are known to exhibit electromechanical coupling under the application of electric fields and imposed deformation [1, 2]. Compared to other types of electromechanical transducers, such as piezoelectric materials, ionomeric transducers have the advantage of high-strain output (>1% is possible), low-voltage operation (typically less than 5 V), and high sensitivity in charge-sensing mode.

One of the salient features of ion-exchange membranes is selective ion conduction. Ion-exchange membranes are polyelectrolytes which contain charged sidegroups covalently bound to the polymer chain. This property leads to charge aggregation within the material and phase separation between hydrophilic 'clusters' containing the charged sidegroups and the hydrophobic backbone. The charge aggregation also leads to a ionic selectivity in which only certain charged groups, either cations or anions, can be transported through the material.

Ion conduction is known to play an important role in the electromechanical transduction of ionomeric polymers. The conduction of ions was identified in Shahinpoor *et al.* [2] as the reason for bending upon application of an electric field, and de Gennes *et al.* [3] proposed a model that related pressure and velocity within the material to electric field and charge flux. This model is similar to form as one developed and experimentally verified by Newbury and Leo [4–6], although Newbury and Leo used force, displacement, charge, and voltage as the state variables for the model. The steady-state distribution of charge due to ionic conduction was determined by Nemat-Nasser and Li [7], where he showed that application of an electric field produces an accumulation of positive charge at one surface and a depletion of cations at the opposite surface. A similar model was recently proposed by Farinholt and Leo [8] to model charge sensing in ionomeric materials. Recently, Nemat-Nasser [9] combined his model of charge redistribution within the material with a model that coupled the charge state within the polymer to the mechanical deformation. This model was able to predict the

\*Author to whom all correspondence should be addressed.

low-frequency relaxation that occurs in certain polymers upon application of a constant electric field.

There is increasing evidence in the literature for a link between charge accumulation and mechanical deformation in ionomeric materials. The deflection response of ionomeric transducers of various compositions and cation forms was recently studied by Nemat-Nasser and Wu [10]. Their results highlighted the relationship between the total charge flow in the polymer to the motion generated at the tip of the transducer. For transducers that utilized Flemion as the ionomer (a commercial polymer from Asahi Glass), Nemat-Nasser and Wu [10] demonstrated a linear relationship between normalized deflection (tip deflection relative to length) versus normalized charge (charge transported versus total fixed charge). Nafion-based transducers exhibited relaxation when subjected to a DC voltage, thus complicating the analysis of the deflection-to-charge analysis. A thorough study of the electromechanical response of Nafion and Flemion in various cation forms was also performed by Asaka *et al.* [11]. They reported that the ‘charge-specific displacement’, defined as the ratio of tip deformation to induced charge, varied as a function of cation form for both ionomers. The charge-specific displacement was then related to the conductivity and freezable water content of the polymer. Nafion is a rubbery material, while BPSH and PATS have the characteristics of engineering thermoplastics.

In this paper we explore the relationship between ion conduction and electromechanical coupling through a series of experiments on three different types of ionomeric materials. The materials studied consist of Nafion, a product of DuPont and one of the most widely studied materials associated with ionomeric transducers, and two alternative ion-conducting polymers, BPSH (sulfonated poly(arylene ether sulfone)) and PATS (poly(arylene thioether sulfone)), that are synthesized by the McGrath group using direct polymerization of sulfonated monomers. This synthetic scheme affords precise control of the amount and the location of ionic groups along the polymer backbone. These polymers differ from Nafion in two major aspects. First, the concentration of ionic groups on a mass basis is almost double that of standard Nafion, 1.70 meq/g for BPSH-40 versus 0.91 meq/g for Nafion 1100. Also, the backbone of the BPSH and PATS copolymers are much stiffer than Nafion, which produces a higher modulus material.

In contrast to the work performed by Nemat-Nasser and Wu [10] and Asaka *et al.* [11], our experimental investigations will focus on the response of the polymers at frequencies greater than approximately 1 Hz. The bulk of the research performed on these materials has concentrated on analyzing the time domain response of the material to various waveforms. As pointed out in Nemat-Nasser and Wu [10], relaxation in some ionomers and in certain cation forms can complicate the charge-to-deflection relationships. For this reason we will utilize frequency response methods to characterize the transducers at frequencies of 1 Hz to approximately 200 Hz. As we will see, analysis of the response at frequencies higher than 1 Hz produces repeatable re-

sults and allows us to define a consistent relationship between mechanical deformation and induced charge.

The paper is organized as follows. The next section discusses fundamental models of charge accumulation in ionomeric materials. This model is used to define a simple representation of the charge accumulation that occurs due to blocking electrodes in the transducer. The section that follows is a detailed description of the methods used to fabricate the transducers and the experiments used to characterize the transducers. The final section is a discussion of the experimental results and conclusions of the paper.

## 2. Surface charge accumulation in ionomeric materials

Ion conduction is measured by applying a voltage to the polymer and measuring the resulting current flow. The relationship between imposed voltage,  $V$ , and current produced,  $I$ , is expressed as the impedance of the material,  $Z$ ,

$$\frac{V(j\omega)}{I(j\omega)} = Z(j\omega) = Z'(\omega) + jZ''(\omega), \quad (1)$$

where  $\omega$  is the frequency of the applied voltage in rad/sec and  $j$  is the imaginary number. The dielectric properties of the material can be studied by transforming the impedance into a relationship between charge,  $Q$ , and voltage,

$$\frac{Q(j\omega)}{V(j\omega)} = \frac{1}{j\omega Z(j\omega)} = C(j\omega), \quad (2)$$

The variable  $C(j\omega)$  represents the measured complex capacitance of the polymer. The complex capacitance can be separated into real and imaginary components

$$C(j\omega) = C'(\omega) - jC''(\omega), \quad (3)$$

where the real part represents capacitive storage and the imaginary component represents loss. The measured complex capacitance is related to the complex permittivity through the expression [12]

$$\varepsilon(j\omega) = \frac{C(j\omega)t}{\varepsilon_0 A} = \varepsilon'(\omega) - j\varepsilon''(\omega), \quad (4)$$

where  $t$  is the sample thickness,  $A$  is the surface area of the electrode, and  $\varepsilon_0$  is the vacuum permittivity.

The dielectric properties are used to characterize the ionic conduction properties of the polymer. For pure insulators, the complex permittivity yields information about the dielectric relaxations of the polymer [12]. Dielectric relaxation measurements in ion-exchange membranes have been performed by a number of researchers. Mauritz and co-workers presented a thorough study of dielectric relaxations in ion-exchange membranes [13, 14]. They noted a power-law dependence of the complex permittivity as a function of frequency [15] and related this characteristic to long range

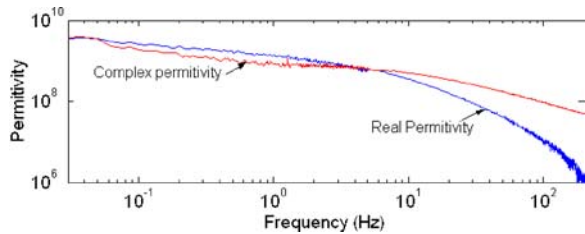


Figure 1 Real and complex permittivities of a typical Nafion-based ionic polymer transducer.

ion transport within the material. Impedance measurements performed by Cahan and Wainwright [16] indicated that this power-law dependence was really an artifact of ‘blocking electrode’, or, ‘space charge’ effects at the polymer-electrode interface. The relationship between electrode effects and dielectric measurements was also studied by Fontanella *et al.* [17] and their results independently confirmed the analysis of Cahan and Wainwright [16]. Further studies by Wintersgill and Fontanella [18] demonstrated that the ionic conduction mechanism was strongly affected by water content and that the low-frequency (less than 100 Hz) power law dielectric behavior was strongly affected by blocking electrode and space charge effects.

Shown in Fig. 1 is the real and complex permittivities of a typical Nafion-based ionic polymer transducer fabricated by our research group. These measurements are consistent with those published by Mauritz *et al.*, for hydrated Nafion in various cation forms. The significant feature of the data is the large low-frequency permittivity exhibited by the polymer; relative permittivity values on the order of  $10^9$  to  $10^{10}$  are not uncommon for ionomeric polymers.

The large low-frequency permittivity is attributed to charge accumulation at the electrodes due to ionic conduction. This was discussed clearly in Wintersgill and Fontanella [18] through examination of the dielectric response of ‘dry’ and ‘wet’ Nafion samples. Wintersgill and Fontanella [18] performed several tests and demonstrated that the apparent ionic conductivity changed dramatically depending on sample size. They attributed this size-dependent variation to the existence of charge accumulation and ‘blocking electrode’ effects at the interface between the polymer and the electrode.

A common model of ion conduction that incorporates blocking electrode effects is shown in Fig. 2. The

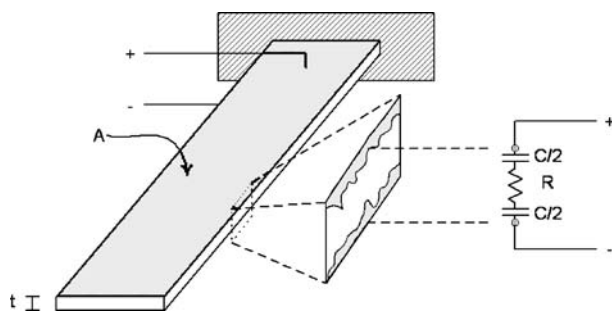


Figure 2 Blocking electrode model using a resistor and two capacitors in series.

polymer is modeled as a pure resistance with capacitors placed in series to account for charge accumulation at the surface. Assuming this model for ion conduction results in the impedance function,

$$Z(j\omega) = R + \frac{1}{j\omega C}, \quad (5)$$

where the imaginary part of the impedance is related to the capacitance of the blocking electrode. This conduction model leads to the relationship

$$\frac{C(\omega)}{A} = \frac{\varepsilon'(\omega)}{t} \quad (6)$$

for the areal capacitance. The frequency-dependence of the capacitance has been added to the function due the measured variation in the dielectric behavior as a function of frequency. In a later section of the paper we will related the areal capacitance to the electromechanical transduction properties of the polymers.

### 3. Experimental methods

This section will discuss the electromechanical measurements used to characterize the ionic polymer transducers, and the methods and optimizations used for their preparation.

#### 3.1. Transducer preparation

Nafion 117 (1100 equivalent weight, 7 mils (178  $\mu\text{m}$ ) thick) membranes are used as the control material for this study. Nafion membranes are commercially available from DuPont and Nafion’s chemical structure is shown in Fig. 3a.

Two experimental ion exchange polymers are also investigated in this study. The two polymers are sulfonated poly(arylene ether sulfone) or BPSH [19], and sulfonated poly(arylene thioether sulfone) or PATS [20]. The chemical structures of BPSH and PATS are shown in Figs 3b and c, respectively. The number following BPSH or PATS represents the number of sulfonic acid groups attached to the polymer backbone (IEC). Both BPSH and PATS membranes were solvent cast from N,N-dimethylacetamide. Details on membrane preparation are found in Kim *et al.* [21]. The advantages of BPSH and PATS copolymers include larger modulus than Nafion when hydrated and an ion content that can be precisely controlled during the copolymer synthesis. A comparison of the general physical properties of Nafion, BPSH, and PATS copolymers is given in Table I.

The electrodes are fabricated on the polymers using an impregnation-reduction method. The impregnation reduction method consists of three main steps; the first is to soak the polymer in a metal salt solution such as  $\text{PtNH}_3\text{Cl}_2$  to populate it with a reducible metal [22]. The next step is to reduce the metal salt on the surface of the membrane. The third step is to electroplate the polymer composite with a thin (50 nm to 100 nm) of gold to increase the surface conductivity. A fourth optional step

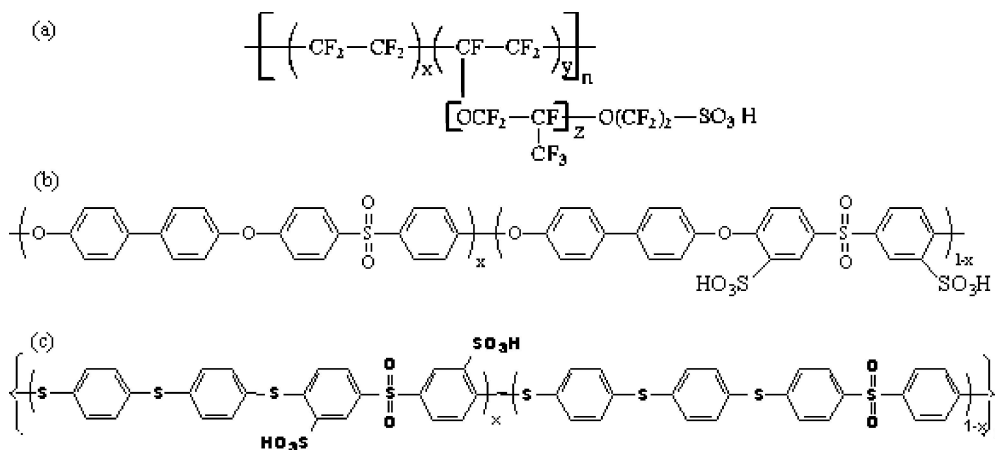


Figure 3 (a) Chemical Structure of Nafion, (b) Chemical Structure of BPSH, (c) Chemical Structure of PATS.

is to perform ion exchange, such as exchanging  $\text{Na}^+$  for the  $\text{Li}^+$  ion. Ion exchange is performed by soaking the polymer in an  $\text{NaOH}$  or  $\text{LiOH}$  solution.

The main parameters optimized in the impregnation-reduction process are the concentration of the reducing agent, the time delay between the increase of reducing agent concentrations, and the number of plating layers. The platinum salt used is a 0.01M  $\text{PtNH}_3\text{Cl}_2$  solution, and the reducing agent is  $\text{NaBH}_4$ . The concentration of the reducing agent is increased with time. The initial concentration of reducing agent used for Nafion is 0.05% w/w, and then another 0.05% w/w  $\text{NaBH}_4$  salt is added every 30 min [22]. When attempting this method on BPSH 35, a concentration of 0.05% w/w proved to rapidly reduce the platinum on the surface, and decrease the penetration of the electrodes into the polymer. Rapid

reduction leads to the reduction of some platinum outside the polymer membrane, which is detrimental to performance.

The second parameter varied is the interval between the increase of reducing agent concentrations. For Nafion an interval of 30 min is used. Intervals of 15 min and 1 h are investigated but the results did not vary significantly from the results using a 30 minute interval. The last parameter varied is the number of plating layers. As discussed in Oguro et al. [23], the actuation strain per unit voltage increases with increasing number of platinum layers until the mechanical stiffness of the electrode reduces the deflection. This increasing trend suggests better performance with increasing the number of plating layers. Although Oguro et al. [23] indicated that five layers produce the optimal bending performance, the optimal number of plating layers has not been verified for BPSH and PATS. In order to reduce the number of variables and save time on each iteration, four platinum layers are used for all polymers. The optimized reducing agent concentrations for each polymer are reported in Table II.

The surface resistivity results are reported in Table II. Surface resistivity is measured using a Guardian Manufacturing four point probe surface resistivity meter (SRM-232). Apart from the BPSH 30 and PATS 40, all the surface conductivity measurements fall below  $1 \Omega/\text{sq}$  after the addition of the platinum layers. A gold overlayer is then electroplated on the platinum surface. This gold layer reduces the surface conductivities of all the transducers below  $0.5 \Omega/\text{sq}$ .

TABLE I Properties of Nafion, BPSH, and PATS copolymers

	EW (g/eq)	IEC (meq/g)	Water uptake (wt %) [19]	Protonic conductivity (S/cm) [27]	Hydrated modulus (MPa) [27]
Nafion 117	1100	0.91	22	0.11	120
BPSH 30	1110	1.3	29	0.06	920
BPSH 35	770	1.53	40	0.08	640
BPSH 40	650	1.7	56	0.10	400
PATS 30	860	1.17	20	0.06	1040
PATS 40	660	1.51	86	0.11	400

EW = Equivalent Weight.

IEC = Ion Exchange Capacity.

Water Uptake, Protonic Conductivity, and Hydrated Modulus determined in liquid water at  $30^\circ\text{C}$ —see indicated references for experimental methods.

TABLE II Fully hydrated transducer thickness, optimal reducing agent concentration, and platinum layers surface conductivity before and after gold electroplating for each ionomer

Ionomer	Transducer thickness ( $\mu\text{m}$ )	Optimal reducing agent concentration % (w/w)	Surface resistivity before electroplating ( $\Omega/\text{sq}$ )	Surface resistivity after electroplating ( $\Omega/\text{sq}$ )
Nafion 117	200	0.05	<1	<0.5
BPSH 30	170	0.01	2.2	<0.5
BPSH 35	190	0.01%	0.6	<0.5
BPSH 40	195	0.005%	0.9	<0.5
PATS 30	180	0.003%	0.9	<0.5
PATS 40	140	0.002%	>8	<0.5

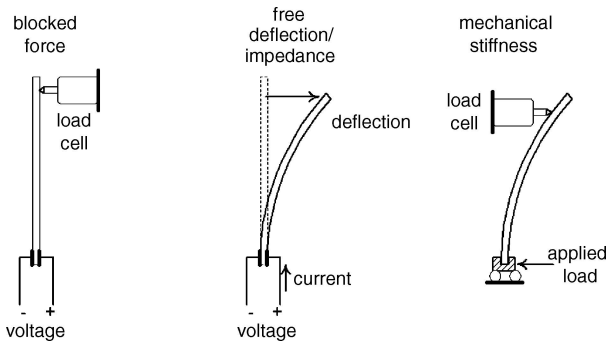


Figure 4 The experimental setup used to for the electromechanical measurements.

The samples are cut into rectangles 30 mm in length and 5 mm in width. The transducers are clamped between the fixture electrodes for all the tests, which results in a free length is 20 mm throughout the experiments. The thickness of the unplated polymer films varied from 0.13 mm to 0.19 mm, and the thickness of the plated transducers varied from 0.14 mm to 0.20 mm. Controlling the thickness of the membranes is difficult to achieve due to the nature of the solvent casting procedure.

### 3.2. Electromechanical measurements

The electromechanical response of the transducers are characterized as actuators using four sets of experiments. Representations of the four tests are shown in Fig. 4. The first test is a blocked force test which characterizes the maximum force the actuator generates due to an applied voltage. In this experiment the tip of the polymer is blocked by a load cell which measures the force generated due to the voltage applied on the electrodes. In the second test the load cell is removed and a laser vibrometer measures the maximum deflection of the transducer in response to an applied voltage. This is the free deflection test. During the free deflection test the current flow to the polymer is also measured allowing the measurement of the electrical impedance of the polymer. The final test performed on the ionic polymers determines the mechanical impedance. In this test one end of the transducer is mechanically displaced by an external shaker, while the other end is blocked with a load cell. Dividing the measured force by the displacement results in the stiffness of the polymer.

The measured data is then post-processed to compute the material parameters of the samples. The strain is computed from the free displacement using the following equation,

$$S = \frac{Dt}{L^2}, \quad (7)$$

where  $S$  is the strain,  $D$  is the measured tip displacement,  $t$  is the average thickness of the polymer, and  $L$  is the free length. This computation assumes that the transducer is in cantilevered beam configuration.

In both actuation tests the actuation current and voltage are measured to compute the electrical impedance of the transducer. The capacitance per unit area is com-

puted from,

$$C = \frac{10^3}{L_t * w * \text{Im}(Z) * \omega} \left( \frac{\text{mF}}{\text{cm}^2} \right), \quad (8)$$

where  $L_t$  is the total length of the polymer in cm and  $w$  is the width in cm,  $\omega$  is the frequency in rad/s, and  $\text{Im}$  is the imaginary part of the impedance. This equation assumes that the polymer is modeled as a capacitor in series with a resistor as discussed earlier in the paper.

Assuming that the polymer is a sliding-pinned beam, the Young's modulus of elasticity is approximated to the first mode using the following Equation [24],

$$E = \frac{kL^3}{\left(\frac{\pi}{2}\right)^3 \left(\frac{wt^3}{12}\right)}, \quad (9)$$

where  $k$  is the measured stiffness,  $L$  is the free length,  $w$  is the width, and  $t$  is the thickness. Franklin [24] showed that the experimental apparatus used in this study is only valid at frequencies lower than 30 Hz. Above this frequency some fixture dynamic effects will deteriorate the accuracy of the FRFs (Frequency Response Function).

All of the experiments performed for this work were analyzed in the frequency domain. This analysis proved to be robust and repeatable for ionic polymer transducers. The input for this test is a random white noise signal of a frequency range from 0 to 256 Hz. An anti-aliasing filter is used to filter the response above 200 Hz. Data in the frequency range of 200–256 Hz is considered distorted by the anti-aliasing filter and consequently it is removed from the analysis. The response is then transformed to the frequency domain using the Fourier transform to yield the frequency response function between the relevant input-output pair.

### 3.3. Experimental results

The experimental methods described in the previous section of the paper are used to characterize a series of ionomeric polymer transducers fabricated from Nafion, BPSH, and PATS. Fig. 5 shows the amplitude of the free deflection frequency response function (FRF) of five transducers fabricated from BPSH and PATS and compared to a Nafion-based ionic polymer transducer. This FRF represents the  $\mu$ strain per unit volt as a function of frequency in the range of 1 to 200 Hz. In the frequency range below 10 Hz, the strain per unit volt is approximately constant and the values range from 80 microstrain/volt to approximately 300 microstrain/volt for BPSH 35. The free deflection FRF exhibits a strong frequency dependence near the resonance of the transducer. Resonance frequencies for the six transducers are in the range of 20 to 60 Hz. All the polymers apart from PATS 40 had higher resonance frequencies compared to that of the Nafion transducer. The higher resonance is due to the increased stiffness of the polymer and less water uptake.

The stiffness of the polymer is measured and the modulus is computed using Equation 9. The results are summarized in Table III for each of the transducers.

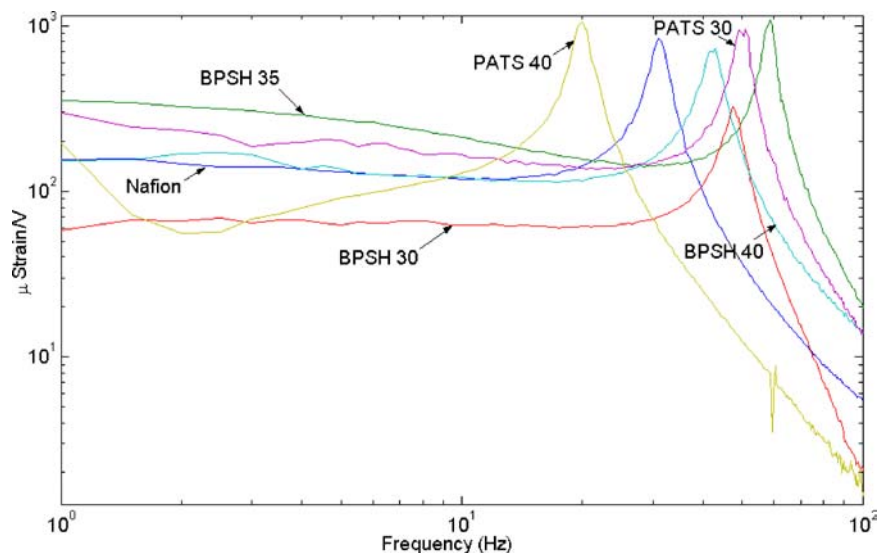


Figure 5 Strain per unit volt of the BPSH and PATS transducers compared to Nafion.

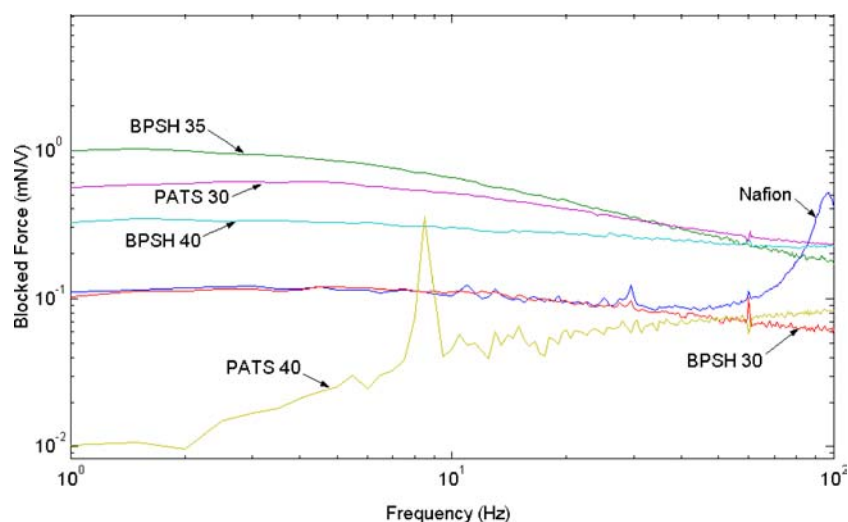


Figure 6 Blocked force per unit volt of the BPSH and PATS polymers compared to Nafion.

The results demonstrate that the modulus of the BPSH materials is approximately twice that of Nafion. The modulus values for the materials are consistent with previously published data [25]. Note that the modulus results shown in Table III differ from the ones shown in Table I since the polymers are in the lithium cation form and they have a stiff platinum electrode on the surface.

The increased modulus of the BPSH materials is also reflected in the measured blocked force. The frequency response functions of the blocked force per unit volt for

the six transducers are shown in Fig. 6. The measured blocked force for the transducer sizes studied are in the range of 0.1 to 1.0 mN/V except for the PATS 40 sample. The BPSH 35 transducer produced the largest blocked force of slightly greater than 1.0 mN/V at frequencies below 10 Hz. The blocked force output of all of the transducers exhibited a slight frequency dependence.

The measured impedance functions of the transducers are shown in Fig. 7. All of the transducers exhibit capacitive behavior at low frequencies and approximately resistive behavior at higher frequencies. The impedance of the materials is between 5 and 100  $\Omega$  for frequencies between 1 and 100 Hz.

TABLE III Values for the stiffness and the Young Modulus estimated using Equation 9

Polymer	Stiffness (N/m)	Young modulus (MPa)
BPSH 30	1.29	1580
BPSH 35	1.86	1276
BPSH 40	0.98	624
PATS 30	1.40	1211
PATS 40	0.11	115
Nafion	0.74	511

### 3.4. Discussion of results

Electromechanical measurements on the polymer transducers demonstrate that the BPSH materials produce the highest strain and blocked force per unit voltage of any of the materials studied. The BPSH 35 material produces approximately 300 microstrain/volt of free deflection and approximately 1 mN/V of blocked force for the sample sizes studied in this work.

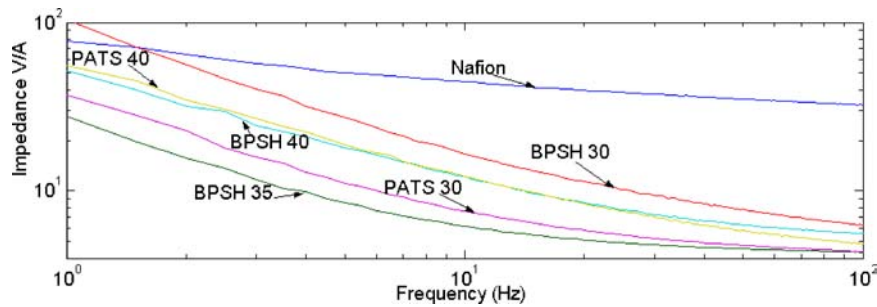


Figure 7 Impedance of the novel polymers compared to Nafion.

One of the primary objectives of this work is to study the relationship between polymer properties and transducer performance. Originally we had hypothesized that the ion-exchange capacity of the polymer or its conductivity would be strongly correlated to any variations we would see in the transducer performance. Unfortunately these trends did not emerge from the results of our study. For example, BPSH 35 is found to have the highest free deflection and blocked force, yet it has a lower conductivity than Nafion 117, BPSH 40, and PATS 40, and its ion-exchange capacity is smaller than BPSH 40.

Very clear trends do emerge when the transducer performance is correlated to the measured capacitance of the material. The frequency-dependent capacitance of the material is computed using Equation 8 from the measured impedance of the sample and is displayed in Fig. 8. As discussed earlier in the paper, the capacitance of the material varies as a function of frequency. At low frequencies the values are on the or-

der of 1 to 10 mF/cm<sup>2</sup> and become smaller at higher frequencies.

Fig. 5 illustrates that the strain produced per unit voltage varies substantially as a function of the base polymer below approximately 10 Hz. If we transform these measurements into strain per unit charge using the expression

$$\frac{S(j\omega)}{Q(j\omega)} = j\omega \frac{S(j\omega)}{V(j\omega)} Z(j\omega) \quad (10)$$

where  $S(j\omega)/V(j\omega)$  is the measured strain per unit volt and  $Z(j\omega)$  is the measured impedance, we see that the variation in the strain response between the different polymers tested is reduced substantially. Fig. 9 is a plot of the strain per volt and strain per charge response over the frequency range 1 to 12 Hz for all of the polymers tested except for PATS 40, which suffered problems in the plating process. Each of the plots is normalized by

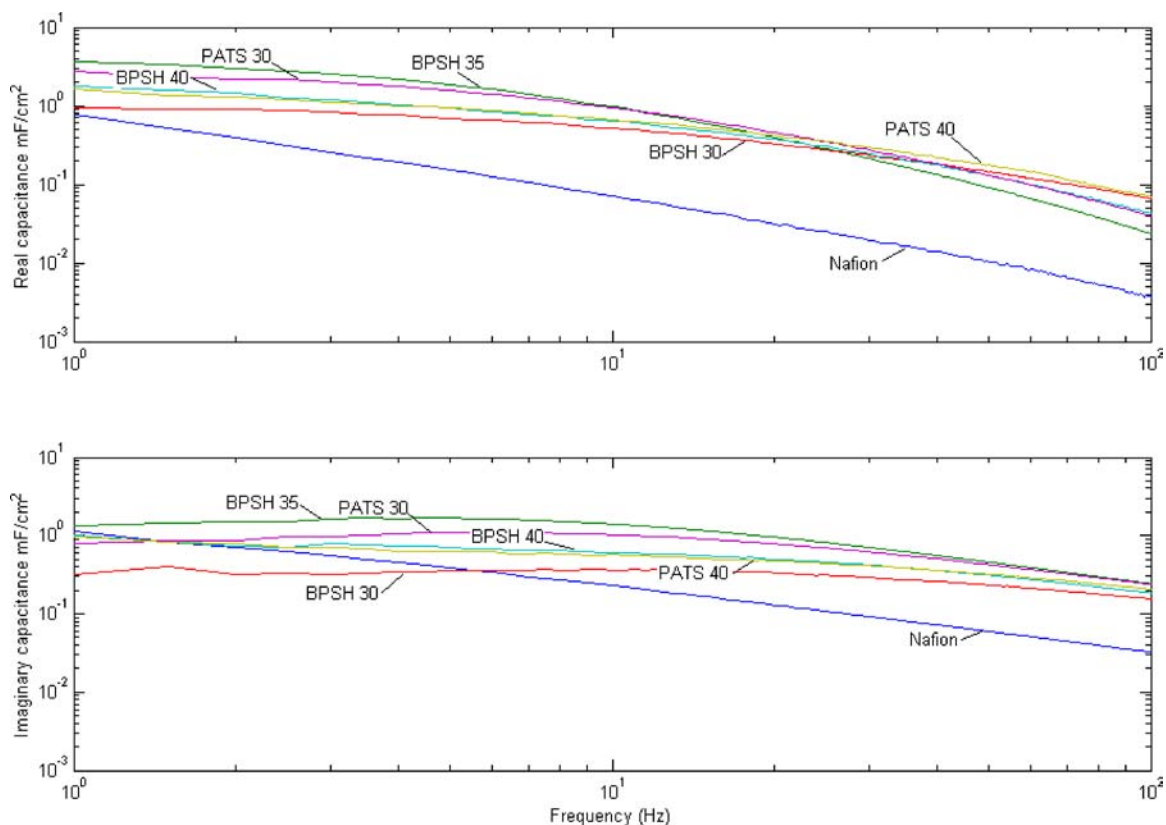


Figure 8 Real and imaginary FRF of the capacitance per cm<sup>2</sup> of the novel polymers compared to Nafion.

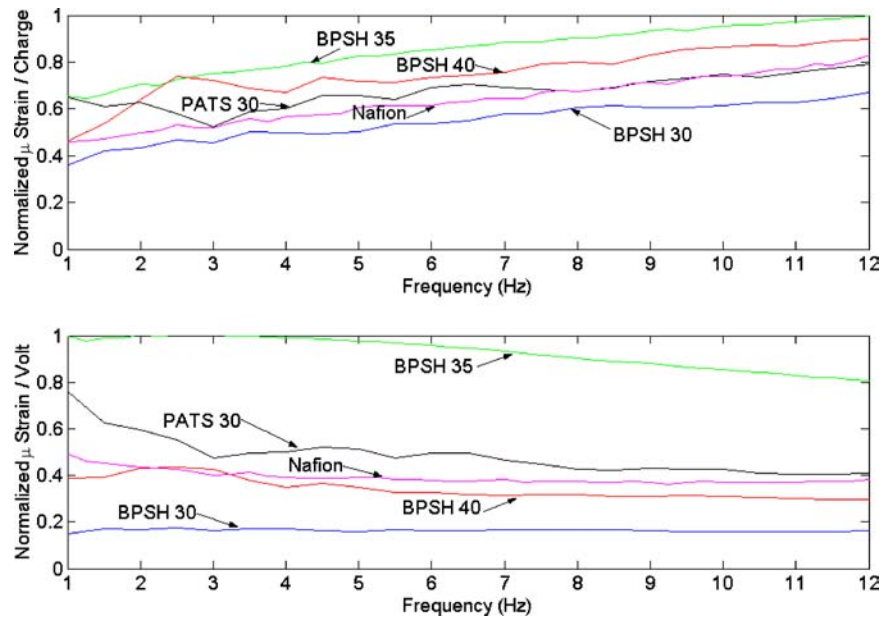


Figure 9 Normalized microstrain per unit charge and normalized microstrain per unit volt for several ionomer transducers.

the maximum value of the response for any polymer at any frequency, thus, all of the values lie between 0 and 1 over the frequency range.

We see in the bottom plot in Fig. 9 that at each frequency, there is between a five-fold (5X) and ten-fold

(10X) variation in the strain per volt between the different transducers tested. Normalizing the strain to the charge induced in the polymer as shown in the top plot, we see that the variation at any frequency is reduced to approximately 1.5X at any frequency.

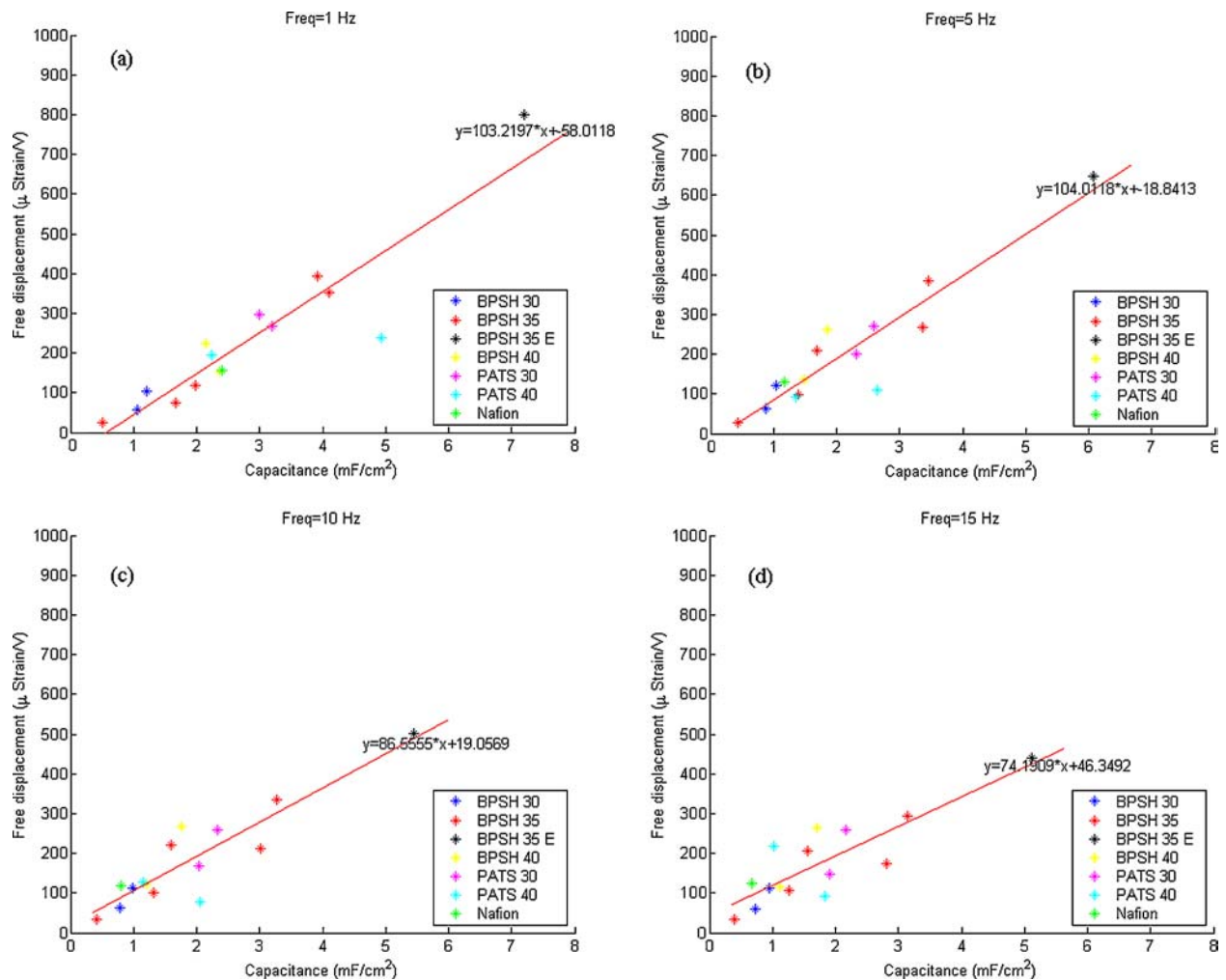


Figure 10 MicroStrain vs. capacitance/cm<sup>2</sup> of each polymer (a) at 1 Hz, (b) at 5 Hz, (c) at 10 Hz, and (d) at 15 Hz.



TABLE IV Microstrain per normalized charge for various ionomer actuators

Polymer	$\frac{\mu\text{strain}}{\frac{C}{m^2}}$
BPSH 35	15.21
BPSH 30	9.83
BPSH 40	13.76
PATS 30	11.90
Nafion	11.83
Nafion (Asaka)	14.58
Flemion (Asaka)	15.48

This analysis demonstrates that the large variation in strain output as a function of voltage is primarily due to the large variation in the voltage-to-current relationships for the polymers tested. Once the results are normalized with respect to charge instead of voltage, then the performance variation in the polymers decreases substantially at the low-frequency range of the tests.

Clear trends also emerge when the strain per unit voltage is compared to the measured capacitance of the material. Fig. 10 is a plot of the measured strain per unit voltage as a function of the measured capacitance for four different frequencies. Each data point represents a particular polymer sample tested during the optimization of the plating process as discussed earlier in the paper. The Figure demonstrates that, at each frequency, there is a linear relationship between the capacitance and the strain output.

The slope of the linear fit to the data shown in Fig. 10 has important physical significance. The units of the slope are microstrain/charge/area, which is equivalent to the average strain produced in the polymer normalized with respect to the electrical displacement induced by the voltage. This parameter can also be computed from the measured data for the polymers tested in this work. Table IV summarizes these results and shows that the strain per unit electric displacement is between 9 and 15 for all of the polymers tested. Once again, we see that normalizing the strain response as a function of charge tends to demonstrate consistent performance between the polymers tested.

It is interesting to compare the results obtained in this work to experimental investigations previously published in the literature. Recently, Asaka *et al.* [26] investigated the performance of Nafion-based and Flemion-based ionomeric transducers as mechanical actuators. In their work they computed the charge-specific displacement, defined as the displacement of the actuator tip to the charge induced by the voltage (in units of mm/C), for Nafion and Flemion actuators with different cations. For lithium as the cation (which is used in this work), their data can be analyzed to compute the strain produced as a function of the electric displacement.

The results of this comparison are shown in Table IV in addition to the data from this work. The results illustrate that Asaka's result is consistent with the data obtained in our analysis. It is important to note that the results summarized in Table IV are listed for four different ionomer materials, with widely different polymer

properties, yet the strain per unit electric displacement is between approximately 10 and 15  $\frac{\mu\text{Strain}}{\frac{C}{m^2}}$  for all polymers studied.

#### 4. Conclusions

The strain response of an ionomeric transducer is strongly correlated with the capacitance of the plated material. In this paper, we studied the transducer performance of several different ionomers from three ionomer families. Results demonstrate that there is an approximately linear relationship between strain response per unit voltage and the capacitance of the transducer. This relationship indicates that the strain output per unit electric displacement is approximately constant for all of the polymers tested. Our experiments indicate that this value ranged between 9.8  $\frac{\mu\text{strain}}{\frac{C}{m^2}}$  and 15  $\frac{\mu\text{strain}}{\frac{C}{m^2}}$  for the polymers tested in this work, and that this value was consistent with data presented previously by other researchers.

These results suggest a strong relationship between charge accumulation at the polymer-metal interface and transducer performance. It is known that the low-frequency capacitance of an ionomeric material is due to blocking electrode effects, therefore a strong correlation between capacitance and strain indicates that charge accumulation at the interface between the electrode and the polymer is responsible for mechanical deformation. Although this has been suggested in the literature before, our results demonstrate that the amount of strain produced by this charge accumulation is approximately the same for a wide range of ionomer materials that have substantially different properties.

Future work will include development of transducers with increased capacitance and stiffer ionomer backbone. Increasing the capacitance is supposed to increase the maximum displacement and the stiffness will increase the force output of the transducer.

#### Acknowledgements

This material is based upon work supported by, or in part by, the U.S. Army Research Laboratory and the U.S. Army Research Office under contract/grant number DAAD19-02-1-0275 Macromolecular Architecture for Performance (MAP) MURI.

#### References

1. K. OGURO, Y. KAWAMI and H. TAKENAKA, *J. Microm. Soc.* **5** (1992) 27.
2. M. SHAHINPOOR, Y. BAR-COHEN, J. SIMPSON and J. SMITH, *Smart Mater. and Struct.* **7**(6) (1998) R15.
3. P. DE GENNES, K. OKUMURA, M. SHAHINPOOR and K. J. KIM, *Europhys. Lett.* **50**(4) (2000) 513.
4. K. M. NEWBURY and D. J. LEO, *J. Intell. Mater. Syst. Struct.* **13**(1) (2002) 51.
5. *Idem.*, *ibid.* **14**(6) (2003) 333.
6. *Idem.*, *ibid.* **14**(6) (2003) 343.
7. S. NEMAT-NASSER and J. LI, "Electromechanical Response of Ionic Polymer Metal Composites," in Proceedings of the SPIE, (2000) Vol. 3987, p. 82.
8. K. FARINHOLT and D. LEO, "Modeling of Electromechanical Charge Sensing in Ionic Polymer Transducers." To appear in *Mechanics of Materials* (2002).

9. S. NEMAT-NASSER, *J. Appl. Phys.* **92**(5) (2002) 2899.
10. S. NEMAT-NASSER and Y. WU, *ibid.*, **93**(9) (2003) 5255.
11. K. ASAKA, N. FUJIWARA, K. OGURO, K. ONISHI and S. SEWA, *J. Electroan. Chem.* **505** (2001) 24.
12. V. V. DANIEL, "Dielectric Relaxation" (Academic Press 1967).
13. K. MAURITZ and H. YUN, *ibid.* **21** (1988) 2738.
14. K. MAURITZ and R. FU, *ibid.* **21** (1988) 1324.
15. K. MAURITZ, *ibid.* **22** (1989) 4483.
16. B. CAHAN and J. WAINWRIGHT, *J. Electrochem. Soc.*, **140**(12) (1993) L185.
17. J. FONTANELLA, M. MCLIN, M. WINTERSGILL, J. CALAME and S. GREENBAUM, *Solid State Ion.* **66** (1993) 1.
18. M. C. WINTERSGILL and J. J. FONTANELLA, *Electrochimica Acta* **43** (1997) 1533.
19. F. WANG, M. HICKNER, Y. KIM, T. ZAWODZINSKI and J. MCGRATH, *J. Membr. Sci.* **197** (2002) 231.
20. K. WILES, V. BHANU, F. WANG and J. E. MCGRATH, *Polym. Preprints* **43**(2) (2002) 993.
21. Y. KIM, L. DONG, M. HICKNER, T. GLASS, V. WEBB and J. MCGRATH, *Macromolecules* **36**(17) (2003).
22. K. J. KIM and M. SHAHINPOOR, *Smart Mater. Struct.* **12** (2003) 65.
23. K. OGURO, N. FUJIWARA, K. ASAKA, K. ONISHI and S. SEWA, "Polymer electrolyte actuator with gold electrodes," in Proceedings of the SPIE, (1999) Vol. 3669, p. 63.
24. J. W. FRANKLIN, "Electromechanical Modeling of Encapsulated Ionic Polymer Transducers," Masters Thesis Virginia Tech, 2003.
25. S. NEMAT-NASSER and C. W. THOMAS, in *Electroactive Polymer Actuators as Artificial Muscles* (SPIE Press, Bellingham, WA, 2001) Chapt. 6, p. 139.
26. K. ASAKA, N. FUJIWARA, K. OGURO, K. ONISHI and S. SEWA, *ibid.* **505** (2001) 24.
27. M. HICKNER, Y. KIM, F. WANG, T. ZAWODZINSKI and J. MCGRATH, in Proceedings of the American Society for Composites, Sixteenth Technical Conference (2001) p. 323.

*Received 14 April  
and accepted 19 October 2004*